

# Strain, vortices, and the enstrophy inertial range in two-dimensional turbulence

Kenneth G. Oetzel and Geoffrey K. Vallis  
University of California, Santa Cruz, California 95064

(Received 6 January 1997; accepted 16 June 1997)

The properties of vortices in a strain field are used to construct a phenomenological theory of the enstrophy inertial range in two-dimensional incompressible turbulence. The theory, based in part on the results and behavior of numerical simulations, attempts to combine spectral inertial range theories of the Kolmogorov type with the dynamics of vortex interactions in physical space. It is based on the assumptions that coherent vortices can survive in a turbulent flow if of sufficient strength compared to the background straining field, and that coherent structures feel a mean strain field, independent of their scale. The first assumption is suggested by a result in the theory of uniform elliptic vortices, while the second comes from numerical simulations. The theory employs a single non-dimensional parameter, essentially the ratio between the enstrophy flux and the mean strain, which then characterizes flows from extremely intermittent decaying turbulence to nearly Gaussian passive scalar dynamics. The theory predicts that in forced two-dimensional turbulence, coherent structures reside in a “background” straining field. The coherent vortices will dominate the flow at a sufficiently large scale, with a fairly abrupt transition at a small scale to a flow in which the classical  $k^{-1}$  enstrophy spectrum holds. In this classical region small amplitude vortices do not survive because the (large-scale) straining field is of larger amplitude than the (small-scale) vorticity. The vorticity itself is passively advected in this regime. If the enstrophy flux is very small compared to the enstrophy itself, then the dynamics will be highly intermittent, with a spectrum determined by the spectrum of the vortices themselves, rather than by the dynamics of the enstrophy flux. The theory predicts that at small scales in forced-dissipative two-dimensional turbulence the energy spectrum will obey the classical enstrophy inertial range predictions even though the non-linear interactions remain spectrally non-local. Passive scalar dynamics are predicted to be similar to vortex dynamics, at small scales. Available numerical simulations are consistent with these suggestions. © 1997 American Institute of Physics. [S1070-6631(97)02710-4]

## I. INTRODUCTION

In the inertial range theory of two-dimensional incompressible turbulence one generally assumes that a cascade of either energy or enstrophy develops across a particular range of scales, and that the flux of the cascading quantity across any scale in the inertial range can be determined solely from dynamical variables on that scale. The assumption that the flux depends solely on wavenumber-local quantities (the *locality hypothesis*), namely just the energy spectrum itself and the wavenumber, is central in yielding non-ambiguous predictions of the energy spectrum. In a steady state the flux must be constant in any range that contains no sources or sinks. Using a simple scaling argument for the two-dimensional Euler equation, it is straightforward to derive the now well known spectrum for the enstrophy cascade,

$$E_k = C' \eta^{2/3} k^{-3}, \quad (1.1)$$

where  $\eta$  is the inertial range enstrophy flux,  $k$  is the wavenumber and  $C'$  a dimensionless constant.<sup>1-3</sup> See Kraichnan and Montgomery<sup>4</sup> and Vallis<sup>5</sup> for reviews.

The relationship between the spectrum and the flux involves an implicit closure of the hierarchy of moments: it relates the two-point correlations of the spectrum to the three-point correlations involved in calculating the flux. Although evidently quite a successful theory in three dimensions, inertial range theory, when applied to the two-dimensional

inertial enstrophy range, is less straightforward because of two phenomena observed in direct numerical simulations that introduce substantial difficulties into closures of this sort: non-local interactions<sup>6-8</sup> and intermittence.<sup>9-12</sup>

Non-local interactions are formally a problem for inertial range closure because they potentially introduce an arbitrary dimensionless function [such as  $\ln(k_0/k)$ , where  $k_0$  is some wavenumber] into the inertial range prediction (1.1), therefore allowing arbitrary slopes. Physically, non-locality may result from small-scale eddies interacting with very large scales in producing enstrophy flux. The flux would then depend on the large-scale structure of the turbulence—behavior that is often outside the inertial range. Incorporating non-locality into an inertial range theory is difficult, as scaling theory provides little guide (e.g., see Ref. 13).

One form of intermittence that has been observed is long-lived coherent structures in the turbulent field.<sup>10,11,14-16</sup> The coherent structures make simple closures difficult because, although they store enstrophy and contribute to the spectrum, they persist; they do not break up and cascade to smaller scales. Thus a field of coherent structures will have a much smaller enstrophy flux for a given spectrum than a field with smaller intermittence<sup>17</sup>. That is, if one specifies the enstrophy flux, the strength and spectrum of the coherent structure component of the field remain undetermined. And for the unforced, decaying, case Bartello and Warn<sup>18</sup> show that coherent structures demand modification of classical

similarity theories<sup>3</sup> to be consistent with numerical simulations.

The approach we take toward resolving the evident non-universality of forced-dissipative two-dimensional turbulence is a phenomenological extension of KBL (Kraichnan–Batchelor–Leith) Kolmogorov-type inertial range theory. In addition to the local quantities in KBL, we add one non-local value: the enstrophy density at the peak of the enstrophy spectrum. Since enstrophy density has units of time<sup>-2</sup>, we have formally avoided introducing a new scale to our model. This is justified in part by truncating a simple Taylor series expansion of the terms affecting enstrophy flux, and in part by the simplicity of the resulting model. The model we construct may be considered a “mean-field” model of turbulence, in that we construct a theory based on the interaction of vortices with the *mean* straining field. The resulting analytical theory of the two-dimensional inertial enstrophy cascade is by no means a complete theory; indeed, even though its construction owes much to the observation of the behavior of numerical simulations, it fails to predict the complete behavior of those simulations. Rather, it provides a phenomenological interpretation of coherent structures in two-dimensional flow, and may provide a theoretical context for future progress in the understanding of two-dimensional mixing.

In the next section the basic dynamics of the system under consideration are laid out. Sections III and IV contain most of the theoretical development of the model, and section V contains a comparison with numerical simulations. Section VI concludes.

## II. DYNAMICAL PRELIMINARIES

### A. Enstrophy flux

For two-dimensional incompressible flow the equation of motion may be written in standard notation as

$$\frac{\partial \zeta}{\partial t} + \nabla \psi \times \nabla \zeta = \tau - (-1)^n \nu_n \nabla^{2n} \zeta - \mu \zeta, \quad (2.2)$$

where  $\psi$  is the streamfunction such that  $\mathbf{v} = -\nabla \times \psi \hat{\mathbf{z}}$  and  $\zeta \equiv \nabla^2 \psi$  is the vorticity and  $\tau$  represents forcing. The last term on the right-hand-side is a linear drag (as from an Ekman layer) and the viscous term is generalized to include the possibility of a “hyperviscosity” with  $n > 1$ . We use a hyperviscosity as a simple means to increase the Reynolds number of our numerical simulations over what is possible with a Newtonian viscosity at reasonable resolutions. We then run simulations with multiple values of  $n$  in an attempt to show independence of our results from the exact details of the viscous term.

For this paper, (2.2) will be considered in a square domain with periodic boundary conditions. Given this, it can be transformed to spectral space by defining

$$\zeta_{\mathbf{k}} \equiv \int d^2 \mathbf{x} e^{i \mathbf{k} \cdot \mathbf{x}} \zeta(\mathbf{x}). \quad (2.3)$$

$\psi_{\mathbf{k}}$  and  $\tau_{\mathbf{k}}$  are similarly defined so (2.2) becomes

$$\frac{\partial \zeta_{\mathbf{k}}}{\partial t} + J_{\mathbf{k}}(\psi, \zeta) = \tau_{\mathbf{k}} - \nu_n k^{2n} \zeta_{\mathbf{k}} - \mu \zeta_{\mathbf{k}}, \quad (2.4)$$

where

$$J_{\mathbf{k}}(\psi, \zeta) = \int (\mathbf{k} \times \mathbf{q}) \psi_{\mathbf{q}} \zeta_{\mathbf{k}-\mathbf{q}} d^2 \mathbf{q}. \quad (2.5)$$

The non-linear terms in the vorticity equations conserve both the total energy,

$$E = \int d^2 \mathbf{x} |\mathbf{v}|^2 = - \int d^2 \mathbf{k} \psi_{\mathbf{k}}^* \zeta_{\mathbf{k}}, \quad (2.6)$$

and the total enstrophy,

$$\Omega = \int d^2 \mathbf{x} \zeta^2 = \int d^2 \mathbf{k} |\zeta_{\mathbf{k}}|^2. \quad (2.7)$$

The isotropic energy and enstrophy spectra are defined by

$$E_k = \int_0^{2\pi} d\theta_k \psi_{\mathbf{k}}^* \zeta_{\mathbf{k}} \quad (2.8)$$

and

$$\Omega_k = \int_0^{2\pi} d\theta_k \zeta_{\mathbf{k}}^* \zeta_{\mathbf{k}}, \quad (2.9)$$

where

$$\int_0^{2\pi} d\theta_k \quad (2.10)$$

represents an integral around a circle of constant  $k = |\mathbf{k}|$ .

Multiplying through by  $-\zeta_{\mathbf{k}}^*$  and integrating over an angle yields the enstrophy dynamics,

$$\frac{1}{2} \frac{\partial \Omega_k}{\partial t} + \frac{\partial Z_k}{\partial k} = \mathcal{F}_k - \mu \Omega_k - \nu_n k^{2n} \Omega_k, \quad (2.11)$$

where the enstrophy flux is defined by

$$Z_k \equiv \int_k^\infty \int_0^{2\pi} d\theta_{k'} dk' \zeta_{\mathbf{k}'}^* J(\psi_{\mathbf{k}'}, \zeta_{\mathbf{k}'}), \quad (2.12)$$

and the enstrophy forcing is

$$\mathcal{F}_k \equiv \int_0^{2\pi} d\theta_k \zeta_{\mathbf{k}}^* \tau_{\mathbf{k}}. \quad (2.13)$$

We will consider these values in a time average sufficiently long that they can be treated as constants, and that

$$\left\langle \frac{\partial \Omega_k}{\partial t} \right\rangle = 0. \quad (2.14)$$

We then attempt to close the equation by writing  $Z_k$  in terms of  $k$  and  $\Omega_k$  and solve for the equilibrium spectrum.

### B. Non-locality

We develop an approximate closure justified partially by observations of direct numerical simulations. Consider first how the right-hand-side of (2.12) transports enstrophy to smaller scales. Define the symmetric enstrophy transport function by

$$R(k,p,q) \equiv \int_0^{2\pi} \int_0^{2\pi} \int_0^{2\pi} \frac{1}{2} (q^{-2} - p^{-2}) \times \mathbf{p} \times \mathbf{q} \zeta_{\mathbf{k}}^* \zeta_{\mathbf{q}} \zeta_{\mathbf{p}} \delta_{\mathbf{k}=\mathbf{p}+\mathbf{q}} k \, d\theta_k \, p \, d\theta_p \, q \, d\theta_q, \quad (2.15)$$

which gives the relation

$$Z_k = \int_k^\infty \int_0^\infty \int_0^\infty R(k',p,q) dp \, dq \, dk'. \quad (2.16)$$

The detailed enstrophy conservation property of  $R$ ,

$$R(k,p,q) + R(p,q,k) + R(q,k,p) = 0, \quad (2.17)$$

along with the symmetries of its definition allow us to write (2.16) in the form

$$Z_k = 2 \int_k^\infty \int_0^k \int_0^k dp \, dq \, dk' R(k',p,q) - 2 \int_0^k \int_k^\infty \int_0^\infty dp \, dq \, dk' R(k',p,q). \quad (2.18)$$

In each of the terms of  $Z(k)$ ,  $k$ ,  $p$  and  $q$  are strictly ordered. In the first term  $q \leq p \leq k \leq k'$ , so it represents transfer to smaller scales, from wavenumber  $p$  to wavenumber  $k'$ . In the second term  $k' \leq k \leq p \leq q$ , so the transfer is to larger scales, from wavenumber  $p$  to wavenumber  $k'$ . In each case, there is a third wavenumber involved in the interaction,  $q$ , which we will call the modulation wavenumber. Since no enstrophy is transferred to or from that wavenumber, the enstrophy at that wave number serves purely to determine the flux rate.

The conditional enstrophy flux,

$$Z_k^{(r,\Delta r)} = \begin{cases} 2 \int_k^\infty \int_r^{r+\Delta r} \int_q^k dp \, dq \, dk' R(k',p,q), & r + \Delta r \leq k, \\ 0, & r < k \leq r + \Delta r, \\ -2 \int_0^k \int_r^{r+\Delta r} \int_q^\infty dp \, dq \, dk' R(k',p,q), & r > k, \end{cases} \quad (2.19)$$

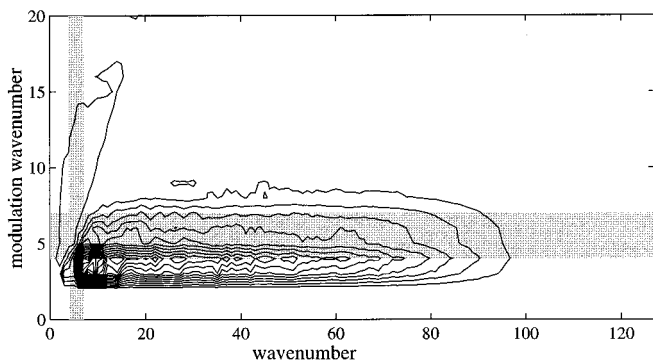


FIG. 1. Contour plot of  $Z_k^{(r,1)}$  for a  $256 \times 256$  simulation, where the vertical axis is  $r$  and the horizontal axis is  $k$ . The forcing wavenumbers are shaded in gray.  $Z$  rolls off at high  $k$  as the enstrophy is removed by viscosity, but is relatively constant in the inertial range.

illustrates how the enstrophy flux depends on the modulation wavenumber. In numerical simulations of the enstrophy cascade, it has been found that most of the enstrophy flux is due to non-local triads.<sup>6-8</sup> In our notation, this means that the areas of strong  $Z_k^{(r,\Delta r)}$  are for  $r \ll k$ . In the absence of any introduced large-scale structure, it is appropriate to study the non-locality in terms of the non-dimensional ratio,  $r/k$ . It is clear from numerical simulations (see Fig. 1) that the characteristic scale of the modulation wavenumber is indeed determined by the forcing scale and the domain size, and is in fact completely unrelated to  $k$  in the inertial range.

The fact that enstrophy flux at all small scales is caused by interactions with the same large scale wavenumbers suggests that one attempt to model turbulence by the interactions of independent small-scale eddies with the same large-scale flow. Because interactions are predominantly non-local, individual eddies do not interact directly, but rather interact only to the degree that each eddy affects the large-scale flow. Given this, one can develop a model of the small-scale dynamics by understanding the interaction of a single eddy with the large-scale strain.

To formalize this, first write  $\mathbf{v} = \mathbf{v}_L + \mathbf{v}_S$  and similarly  $\zeta = \zeta_L + \zeta_S$ , where  $\mathbf{v}_L$  characterizes a large-scale flow,  $\mathbf{v}_S$  characterizes a single-small scale eddy,  $\zeta_L = \nabla \times \mathbf{v}_L$  and  $\zeta_S = \nabla \times \mathbf{v}_S$ . Provided the small-scale eddy is substantially larger than the viscous scale, we can approximate (2.2) by

$$\frac{\partial \zeta_L}{\partial t} + \frac{\partial \zeta_S}{\partial t} \approx -((\mathbf{v}_L \cdot \nabla) \zeta_L + (\mathbf{v}_L \cdot \nabla) \zeta_S + (\mathbf{v}_S \cdot \nabla) \zeta_L + (\mathbf{v}_S \cdot \nabla) \zeta_S) + \tau. \quad (2.20)$$

Since  $\nabla^2$  is predominantly sensitive to small scales,  $(\mathbf{v}_S \cdot \nabla) \zeta_L$  will be much smaller than  $(\mathbf{v}_L \cdot \nabla) \zeta_S$  so it can be dropped in this approximation. Schematically, we can separate (2.20) into the large- and small-scale terms, and examine the evolution of the eddy with

$$\frac{\partial \zeta_S}{\partial t} \approx -((\mathbf{v}_L \cdot \nabla) \zeta_S + (\mathbf{v}_S \cdot \nabla) \zeta_S). \quad (2.21)$$

The non-locality of interactions contributing to enstrophy flux suggests that the  $(\mathbf{v}_S \cdot \nabla) \zeta_S$  term can be dropped. The problem with dropping this term is that the remaining equation,

$$\frac{\partial \zeta_S}{\partial t} \approx -(\mathbf{v}_L \cdot \nabla) \zeta_S, \quad (2.22)$$

simply describes the small-scale dynamics as passive scalar advection, and it is known that vorticity dynamics are different in certain important respects:<sup>19,20</sup> in general, the steady state vorticity will be highly intermittent and exhibit steep spectra, while the passive scalar statistics will be much more Gaussian and are much closer to the  $k^{-1}$  spectrum in the inertial range. We will see that when the velocity field is locally strongly correlated with the vorticity field, that  $(\mathbf{v}_S \cdot \nabla) \zeta_S$  becomes important because it suppresses enstrophy flux. So, while this term never appears in enstrophy flux calculations, it is critical to the formation of coherent structures and steep spectra.

### C. Passive scalar dynamics

The dynamics of a passive scalar  $\phi_{\mathbf{k}}$  are determined by equations similar to those for vorticity dynamics, but the analogue of vorticity (i.e.,  $\phi_{\mathbf{k}}$ ) and the velocity fields are not functionally related. The evolution equation is

$$\frac{\partial \phi_{\mathbf{k}}}{\partial t} + J_{\mathbf{k}}(\psi, \phi) = \tilde{\tau}_{\mathbf{k}} - \nu_n k^{2n} \phi_{\mathbf{k}} - \mu \phi_{\mathbf{k}}. \quad (2.23)$$

To allow spectral comparisons between  $\phi$  and  $\zeta$  we will let  $\tilde{\tau}_{\mathbf{k}}$  and  $\tau_{\mathbf{k}}$  have the same spectrum, but have no correlation in time or phase.

The analog of (2.11) for the passive scalar is

$$\frac{1}{2} \frac{\partial \Phi_k}{\partial t} + \frac{\partial \tilde{Z}_k}{\partial k} = \tilde{\mathcal{T}}_k - \mu \Phi_k - \nu_n k^{2n} \Phi_k, \quad (2.24)$$

where

$$\Phi_k = \int_0^{2\pi} d\theta_k \phi_{\mathbf{k}}^* \phi_{\mathbf{k}} \quad (2.25)$$

is the conserved quantity corresponding to enstrophy and

$$\tilde{Z}_k \equiv \int_0^\infty \int_0^{2\pi} d\theta_k dk' \phi_{\mathbf{k}}^* J(\psi_{\mathbf{k}}, \phi_{\mathbf{k}}) \quad (2.26)$$

is the passive scalar flux. The conserved quantity corresponding to energy is

$$K_k = \int_0^{2\pi} d\theta_k \psi_{\mathbf{k}}^* \phi_{\mathbf{k}}, \quad (2.27)$$

and is a correlation between the passive scalar and the fluid stream function. Since the forcing terms are not correlated, this term will always be zero, and as a result, it does not act as a severe constraint on the flow. In numerical simulations Babiano<sup>19</sup> and Ohkitani<sup>20</sup> have observed shallower spectra in the passive scalar than in vortex dynamics, approaching the classical  $-1$  KBL slope. Also, coherent structures are not observed, at least not to the same degree as in vortex dynamics.

### III. INERTIAL RANGE THEORIES

In an inertial range the forcing, friction and viscosity are negligible, i.e. in (2.11),

$$\tilde{\mathcal{T}}_k - \mu \Omega_k - \nu_n k^{2n} \Omega_k \approx 0. \quad (3.28)$$

If the forcing is band limited, then it has a characteristic scale, say  $k_\tau$ . Since the  $k^2$  in the viscous term biases it toward large wavenumbers, it will preferentially remove enstrophy over energy. Given appropriate choices for  $\mu$  and  $\nu$ , the spectrum will adjust so that the drag term removes energy at small wavenumbers as the flow approaches statistical steady state. In principle, then, there are potentially two inertial ranges; the reverse energy cascade for  $k_\mu < k < k_\tau$  and the enstrophy cascade for  $k_\tau < k < k_\nu$ . In a long enstrophy cascade, the enstrophy flux is constant, and the energy flux is negligible.

In many inertial range theories the steady state enstrophy cascade is essentially described by a closure of the form

$$Z_k = \sigma_k k \Omega_k, \quad (3.29)$$

where  $\sigma_k$  is the rate of strain, considered to be defined by (3.29). In the inertial range, (2.11) reduces to

$$\frac{\partial}{\partial k} Z_k = 0, \quad (3.30)$$

so the enstrophy flux is constant,  $Z_k \equiv \eta$ .

Classic KBL inertial range theory argues that the rate of strain at any scale can only be dependent on the dynamic variables on that scale,  $k$  and  $\Omega_k$ , so by simple dimensional analysis,

$$\sigma_k \propto (k \Omega_k)^{1/2}, \quad (3.31)$$

which results in the classic spectrum

$$\Omega_k = C' \eta^{2/3} k^{-1}, \quad (3.32)$$

which is equivalent to the energy spectrum (1.1).

The numerical non-locality results referred to in Sec. II B suggest that this basic assumption [namely (3.31)] is false. In fact, the enstrophy flux will depend on the dynamical variables near the peak of the spectrum ( $k_\tau$  and  $\Omega_{k_\tau}$ ) as well as the local ones. To extend the KBL model we will include the effect of non-local interactions using the simple assumption that the enstrophy flux at small scales is sensitive to the strength of the large-scale eddies but not their size. In practice this will mean including the enstrophy at the peak of the spectrum,  $k_\tau \Omega_{k_\tau}$ , in the closure. Given this assumption, the most general closure allowed takes the form

$$\sigma_k \propto (k_\tau \Omega_{k_\tau})^{1/2} \Theta \left( \frac{k \Omega_k}{k_\tau \Omega_{k_\tau}} \right), \quad (3.33)$$

where  $\Theta$  is a function representing the effect of the competition between the local and non-local terms in (2.21) on the enstrophy flux.

Because  $\Theta$  is non-linear, it potentially allows more than one solution. In fact, as we will show in the next section, it is reasonable to expect that it has two; one of which we characterize as a coherent structure solution, and the other as a background flow. The detailed analysis of the next section will attempt to explain much of the observed phenomenology through this simple extension of the classical theory.

### IV. PHYSICAL INTERPRETATION OF THE NON-LOCAL THEORY

We consider the spectrally non-local interactions to be dominated by spatially local interactions, between the local vorticity and the velocity. In Sec. IV A we argue that the strain field is the dominant part of the velocity field affecting the small-scale vorticity evolution. In Sec. IV B, we introduce an approximate flow model where the continuous vorticity field is treated as a sum of independent eddies, each interacting with the large-scale strain field. We use a mean strain field approximation somewhat analogous to the mean field theories of statistical mechanics (e.g., Ma<sup>21</sup>) to simplify the problem to where it is analytically tractable. Finally, in Sec. IV C, we use a uniform elliptical vortex (UEV) as an eddy model. The UEV is reduced to a simple parameteriza-

tion of the interaction between the small-scale eddies and the strain field which in turn is applied to the mean strain field theory, resulting in a rather idealized view of turbulence.

### A. Strain

To examine strain rate closure arguments in the context of the non-locality results, the enstrophy flux associated with a localized patch of vorticity or eddy will be given approximately by

$$Z_{\text{eddy}} \sim \int \int_{\text{eddy}} d^2\mathbf{x} \{ \zeta_S(\mathbf{v}_L \cdot \nabla) \zeta_S + \zeta_S(\mathbf{v}_S \cdot \nabla) \zeta_S \}. \quad (4.34)$$

Since the total enstrophy flux at small-scales is just the sum of the flux associated with individual eddies, the assumption that the rate of strain depends purely on the small-scale enstrophy neglects the non-local terms in the calculation of the Jacobian. To include the non-local interactions in a enstrophy flux closure, the interactions between the small-scale structures and the large-scale flow must be parameterized. The integral in (4.34) only covers a small area of the large-scale flow, so we expand the large-scale velocity in a Taylor series about the center of the eddy:

$$\mathbf{v}_L = \mathbf{v}_0 + \Sigma \delta \mathbf{x} + \mathcal{O}(\delta x^2), \quad (4.35)$$

where  $\mathbf{v}_0$  is the large-scale velocity at the eddy center, and

$$\Sigma = \begin{bmatrix} \frac{\partial u}{\partial x} & \frac{\partial u}{\partial y} \\ \frac{\partial v}{\partial x} & \frac{\partial v}{\partial y} \end{bmatrix}_{\mathbf{x} = \text{eddy center}}. \quad (4.36)$$

The first term in the expansion (4.35) corresponds to the linear advection of the eddy, so it does not contribute to the enstrophy flux. The second term splits into two parts: symmetric and antisymmetric. The antisymmetric part of  $\Sigma$  is just the vorticity of the large-scale flow,

$$\Sigma - \Sigma^T = \begin{bmatrix} 0 & -\zeta \\ \zeta & 0 \end{bmatrix}, \quad (4.37)$$

and characterizes the circulation of the flow. Since large-scale circular motion rotates the small-scale eddy, but does not deform it, this term can be neglected as well. The symmetric component, the strain field,

$$S = \Sigma + \Sigma^T, \quad (4.38)$$

characterizes the hyperbolicity of the flow. A hyperbolic flow stretches eddies along an axis and contracts them along the perpendicular axis. This stretching process transfers enstrophy to smaller scales as the eddy gets thinner along the contracting axis. Since the higher order terms in (4.35) decay away as the eddy gets small, we expect that the strain field will be the primary contributor to nonlocal enstrophy flux.

Since we are primarily interested in isotropic turbulence, we shall describe the strain with a quantity which is independent of the axis. To do that, we use  $s^2 \equiv -\det S$ . Weiss<sup>22</sup> used the complex quantity

$$\lambda = \left( \frac{\partial u}{\partial x} - \frac{\partial v}{\partial y} \right) + \left( \frac{\partial u}{\partial y} + \frac{\partial v}{\partial x} \right) i, \quad (4.39)$$

for strain, which for incompressible flow is related to  $s$  by

$$s^2 = |\lambda|^2. \quad (4.40)$$

Weiss (1991) showed that in wavenumber space, the relation between the enstrophy and the strain is purely a phase,

$$\lambda_{\mathbf{k}} = \frac{i(k_x + ik_y)}{k_x - ik_y} \zeta_{\mathbf{k}}, \quad (4.41)$$

which means that in a domain with no net circulation, the total enstrophy is equal to the total squared strain:

$$\int \int \zeta^2 d\mathbf{x} = \int \int s^2 d\mathbf{x}. \quad (4.42)$$

In physical space the effect of the phase is to smear out the strain relative to the enstrophy. For instance, the strain field around a delta function of vorticity decays away only as  $r^{-2}$ . This means that the relationship between the strain field and the vorticity field is spatially non-local.

If one considers an eddy to be a structure with spatially compact vorticity, then eddies will interact with one another mostly through long range strain–vorticity interactions. When one is examining spatially local structures, the decomposition of the stream function into large- and small-scale parts is not unique. Nonetheless, as the the small scales are accentuated by the derivative relating vorticity to velocity, it is natural to think of them as consisting predominantly of vorticity, and then the large scale as consisting predominantly of strain and mean flow. In this light, the first term in (4.34) is a strain–vorticity interaction and represents the effect of all other eddies on the local one. The second term is a vorticity–vorticity interaction, and represents the eddy self-interaction.

In terms of the enstrophy of the local eddy,  $\Omega_{\text{eddy}}$ , the terms in (4.34) should scale as

$$Z_{\text{eddy}} \sim s \Omega_{\text{eddy}} + \Omega_{\text{eddy}}^{3/2}. \quad (4.43)$$

If the field is constructed entirely of eddies, then

$$\langle s^2 \rangle = \langle \Omega_{\text{eddy}} \rangle, \quad (4.44)$$

which means that the competition between the two terms is a competition between the local enstrophy and the mean enstrophy. Using the local enstrophy to estimate the mean enstrophy results in the classic spectrum (3.32). Thus, for the spectrum to deviate from the classic one, the local enstrophy must deviate significantly from the mean, implying that it must be highly intermittent. Figure 2 shows typical probability densities for strain and vorticity, indicating that the enstrophy field does deviate significantly from the mean. The vorticity distribution is highly non-Gaussian reflecting its intermittent behavior, whereas the nearly Gaussian strain distribution is clearly not so intermittent.

### B. Spatial intermittence in an inertial range theory

To develop the relationship between spectral enstrophy flux and spatial intermittence, it is useful to simultaneously describe the fields in terms of both position and scale. To do

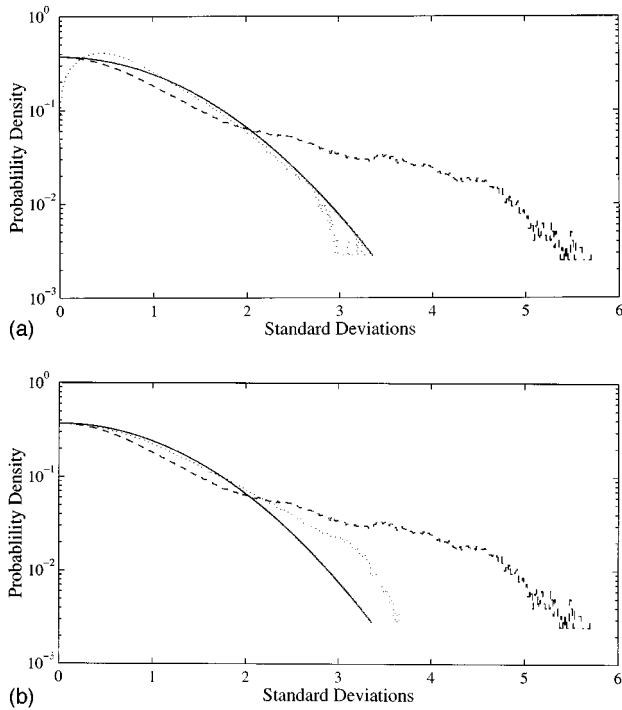


FIG. 2. (a) PDFs of the strain (dotted line) and vorticity (dashed line) compared to a Gaussian (solid line). (b) PDFs of the passive scalar (dotted line) and vorticity (dashed line) compared to a Gaussian (solid line). The PDFs are taken from a time average of data from simulation C, defined in Table I.

this heuristically, we consider the field as a sum of non-overlapping eddies, each of spatially compact support and covering a finite area,  $A$ , and associated with a characteristic inverse scale,  $\alpha$ , such that  $A = \pi\alpha^{-2}$ . Thus,  $\alpha$  is different from the Fourier wavenumber  $k$ , but the two will not be unconnected.

Let  $\mathcal{D}$  represent the spatial domain of the turbulent flow, and normalize the spatial scale so that  $\mathcal{D}$  has unit area. Next, define  $\mathcal{D}_\alpha$  to be the part of  $\mathcal{D}$  covered by eddies with area  $A \geq \pi\alpha^{-2}$  and  $\bar{A}_\alpha$  to be the area of  $\mathcal{D}_\alpha$ . For simplicity, assume that the flow is space filling in the sense that  $\mathcal{D}_\infty = \mathcal{D}$  and  $\bar{A}_\infty = 1$ . Finally, define

$$\bar{\Omega}_\alpha \equiv \int_{\mathcal{D}_\alpha} \frac{1}{2} \zeta^2 d^2A, \quad (4.45)$$

and the total enstrophy,

$$\Omega \equiv \bar{\Omega}_\infty. \quad (4.46)$$

These definitions allow an enstrophy spectrum,

$$\Omega_\alpha \equiv \frac{\partial \bar{\Omega}_\alpha}{\partial \alpha}, \quad (4.47)$$

an area spectrum,

$$A_\alpha \equiv \frac{\partial \bar{A}_\alpha}{\partial \alpha} \quad (4.48)$$

and an intermittence spectrum,

$$\xi_\alpha^2 \equiv \frac{\Omega_\alpha}{\Omega A_\alpha}, \quad (4.49)$$

to be defined. Physically, the intermittence is the ratio of the RMS vorticity of eddies of scale  $\alpha$  to the overall RMS vorticity:

$$\xi_\alpha = \left( \frac{\partial \langle \zeta^2 \rangle_{\mathcal{D}_\alpha}}{\partial \alpha} \frac{\langle \zeta^2 \rangle_{\mathcal{D}}}{\langle \zeta^2 \rangle_{\mathcal{D}_\alpha}} \right)^{1/2}, \quad (4.50)$$

where we use  $\langle \rangle_{\mathcal{D}_\alpha}$  to refer to the average of a quantity over area  $\mathcal{D}_\alpha$ . We will also use  $\langle \rangle$  as a short hand for  $\langle \rangle_{\mathcal{D}}$ , an average over the entire domain. If eddies on the scale  $\alpha$  have a higher enstrophy density than the bulk of the flow, they will have an intermittence greater than one.

Since the relationship between the strain field and the enstrophy field is spatially non-local, it is reasonable to expect that the evolution of a local eddy could depend on the two locally independent dynamical variables; the vorticity and the strain. However, even when the enstrophy field is highly intermittent, the strain field will be much more evenly distributed. Thus we propose a *mean strain field* theory.

The basic approximation of the mean strain field theory is that eddies of all scales statistically see the same strain field, and so the strain field can be characterized in a manner independent of scale. It is made plausible (but not rigorous) because we are treating the strain generated by the eddy itself as part of the eddy self-interaction, meaning the eddy has no direct effect on the strain field it sees. If the mixing of eddies is thorough, then it is not unreasonable to expect that all eddies will sample the large-scale strain field equally.

Given this approximation, the mean enstrophy flux associated with a particular eddy will depend on both its intrinsic enstrophy and the mean strain generated by the entire flow. Since strain and vorticity have the same units, the dynamics will now depend on the non-dimensional ratio  $\zeta^2/\langle s^2 \rangle$ . As noted earlier,  $\langle s^2 \rangle = \langle \zeta^2 \rangle$ , so in fact, this non-dimensional ratio is just the square of the intermittence,  $\xi$ . The analogous enstrophy flux closure to the classic inertial range theories takes the general form discussed in Sec. III [cf. equation (3.29)],

$$Z_\alpha = \alpha \Omega_\alpha \langle s^2 \rangle^{1/2} \Theta \left( \frac{\gamma^2 \Omega_\alpha}{\langle s^2 \rangle A_\alpha} \right), \quad (4.51)$$

where  $\Theta(\gamma^2 \xi^2)$  is an arbitrary function, and  $\gamma$  is a unitless constant which will be discussed further below.

To get the enstrophy conservation equation, compute

TABLE I. Resolutions and parameters of the viscous term [refer to (2.2)].

Simulation	Resolution	$n$	$\nu_n$
A	512×512	1	$4 \times 10^{-4}$
B	512×512	2	$1.7 \times 10^{-8}$
C	512×512	4	$5 \times 10^{-18}$
D	512×512	8	$9 \times 10^{-37}$
E	256×256	4	$1 \times 10^{-15}$

$$\frac{\partial}{\partial \alpha} Z_\alpha = \Omega_\alpha \langle s^2 \rangle^{1/2} \left[ \Theta(\epsilon) - \epsilon \Theta'(\epsilon) \frac{\partial \ln(A_\alpha)}{\partial \ln(\alpha)} + (\Theta(\epsilon) + \epsilon \Theta'(\epsilon)) \frac{\partial \ln(\Omega_\alpha)}{\partial \ln(\alpha)} \right], \quad (4.52)$$

where

$$\epsilon \equiv \gamma^2 \xi^2. \quad (4.53)$$

Let  $a \equiv \ln(A)$ ,  $\omega = \ln(\Omega)$  and  $\kappa = \ln(\alpha)$ , and then (4.52) becomes

$$\frac{\partial}{\partial \alpha} Z_\alpha = \Omega_\alpha \langle s^2 \rangle^{1/2} \left[ \Theta(\epsilon) - \epsilon \Theta'(\epsilon) \frac{\partial a}{\partial \kappa} + (\Theta(\epsilon) + \epsilon \Theta'(\epsilon)) \frac{\partial \omega}{\partial \kappa} \right]. \quad (4.54)$$

Since  $\partial Z_\alpha / \partial \alpha = 0$  the inertial range spectrum,

$$(\Theta(\epsilon) + \epsilon \Theta'(\epsilon)) \frac{\partial \omega}{\partial \kappa} = \epsilon \Theta'(\epsilon) \frac{\partial a}{\partial \kappa} - \Theta(\epsilon), \quad (4.55)$$

ensues. Also, it is easy show from the definition of  $\epsilon$  that

$$\epsilon = \frac{\gamma^2}{\langle s^2 \rangle} e^{\omega - a}. \quad (4.56)$$

Although (4.55) and (4.56) are not a closed set of equations, much can be learned about two-dimensional turbulence in this mean field approach by examining their behavior under various closure assumptions. For instance, if one assumes the eddies are self-similar under scaling, the corresponding closure is  $\Omega \propto A$ , which results in the closed equation,

$$\frac{\partial \omega}{\partial \kappa} = -1. \quad (4.57)$$

Integrating (4.57) to

$$\Omega_\alpha = \Omega_0 \left( \frac{\alpha}{\alpha_0} \right)^{-1}, \quad (4.58)$$

and letting

$$A_\alpha = A_0 \left( \frac{\alpha}{\alpha_0} \right)^{-1}, \quad (4.59)$$

shows that the intermittence is a constant,

$$\xi^2 = \frac{\Omega_0}{\langle s^2 \rangle A_0}, \quad (4.60)$$

and the enstrophy flux is

$$\eta = \Omega_0 \alpha_0 \langle s^2 \rangle^{1/2} \Theta(\gamma^2 \xi^2). \quad (4.61)$$

When the total enstrophy is equal to the mean strain and the total area is one, then the intermittence is one; and there are no coherent structures.

For flows that exhibit intermittence, instead of assuming the self-similar solution one may assume a fixed spectral slope for the area function, so that

$$\frac{\partial a}{\partial \alpha} = g - 1, \quad (4.62)$$

where  $g$  is a constant deviation from the self-similar  $\alpha^{-1}$  slope. Under these circumstances, (4.55) becomes

$$\frac{\partial \omega}{\partial \kappa} = \frac{g \epsilon \Theta'(\epsilon)}{\Theta(\epsilon) + \epsilon \Theta'(\epsilon)} - 1. \quad (4.63)$$

As long as  $g$  is of order one or smaller and the intermittence is of order one, the first term on the right-hand-side of (4.63) will be small, and the whole equation reduces approximately to (4.57). If, on the other hand, the intermittence becomes large, two things happen—the geometric scaling becomes important in the enstrophy spectrum, and, as will be shown later, the root in the denominator  $\Theta(\epsilon_c) + \epsilon_c \Theta'(\epsilon_c)$  can go to zero. This root is a separation point between two very distinct behaviors of two-dimensional turbulence. When  $\epsilon > \epsilon_c$  the flow is highly intermittent and has an enstrophy spectrum that is very sensitive to the geometrical form of the flow. When  $\epsilon < \epsilon_c$ , the flow has moderate to low intermittence and is predicted to have an  $\alpha^{-1}$  spectrum.

### C. Elliptic vortices in a random strain field

The theory of the previous subsection is relatively general, save for the closure assumption itself. This is essentially that the vorticity field can be described as isolated eddies that only interact through the mean strain field; the dynamical behavior can then be described by a single function,  $\Theta(\epsilon)$  [c.f. equation (3.33)]. It is still not a very useful theory, since the form of  $\Theta$  is as yet undetermined. To proceed, we will now make further assumptions as to the nature of the turbulence itself. While in real turbulence the eddy shapes are complicated and varied, we will assume that many of the essential dynamical characteristics can be understood by examining only a very simple class of eddies. In particular, we will use elliptical patches of uniform vorticity as our model eddies because their properties are relatively well understood.<sup>23,24</sup> This is an admitted simplification—the vortices of two-dimensional turbulence are neither perfect ellipses nor uniform. However, the simplification does enable information about the physical properties of vortex interactions to be incorporated into an otherwise purely spectral theory. Furthermore, it is probably more realistic that supposing the turbulent field to be point vortices, an approach which nevertheless has yielded useful information about turbulence.<sup>25</sup>

A uniform elliptical vortex (UEV) is characterized by its minor and major axes,  $a$  and  $b$ , the angle of its major axis to the  $x$ -axis,  $\theta$ , and the vorticity,  $\zeta$ , within the ellipse,

$$1 \geq \frac{(x \cos \theta + y \sin \theta)^2}{a^2} + \frac{(-x \sin \theta + y \cos \theta)^2}{b^2}; \quad (4.64)$$

and the strain field by the rate of strain,  $s$ , where

$$u = -sx, \quad v = sy,$$

and  $u$  and  $v$  are the horizontal and vertical velocities. A notable characteristic of this system<sup>24</sup> is that for  $s < \gamma \zeta$ ,

where  $\gamma \approx 0.15$  there exist both stable and oscillating states for the vortex; but for  $s > \gamma\zeta$  the vortex aligns to the axes ( $\theta \rightarrow 0$ ) and stretches exponentially along the  $y$ -axis, with

$$\dot{a} = -sa \quad (4.65)$$

and

$$\dot{b} = sb. \quad (4.66)$$

At  $s = \gamma\zeta$  there exists a stable state with  $a/b = \epsilon_c \approx 2.89$ . For a theory similar to the classic inertial range theories, we wish to calculate the spectral enstrophy flux associated with this process. To do this, define a spectrum such that all the enstrophy in a particular eddy is associated with the scale

$$\alpha_v = \begin{cases} (ab)^{-1/2}, & a < \epsilon_c b, \\ (\epsilon_c b^2)^{-1/2}, & a \geq \epsilon_c b. \end{cases} \quad (4.67)$$

As an approximation, assume that if  $s < \gamma\zeta$  the eddy is completely elastic; and as a result there will be no associated enstrophy flux. In addition, assume that all the enstrophy associated with a particular eddy is transported to smaller scales as it stretches beyond the elastic limit. Given these assumptions, the behavior of a UEV can be simply parameterized by

$$\eta_v(\alpha) = \Omega_v(\alpha) \dot{\alpha}_v, \quad (4.68)$$

where  $\eta_v$  is the enstrophy flux associated with a single eddy, and

$$\Omega_v(\alpha) = \frac{1}{2} \zeta_v^2(\alpha) A_v(\alpha) \quad (4.69)$$

is the enstrophy associated with the eddy, and

$$A_v(\alpha) = \pi ab \delta(\alpha - \alpha_v) \quad (4.70)$$

is the area of the eddy. Substituting (4.66) and (4.67) into (4.68) gives

$$\eta_v(\alpha) = \begin{cases} 0, & < \gamma\zeta_\alpha, \\ s\alpha\Omega_v(\alpha), & s \geq \gamma\zeta_v. \end{cases} \quad (4.71)$$

We write the individual vortex properties  $\Omega_v(\alpha)$ ,  $A_v(\alpha)$  and  $\eta_v(\alpha)$  as spectra over  $\alpha$  so we can treat  $v$  as an index to all the eddies in a field and sum over them to generate the spectra developed in Sec. IV B. To start, we get the enstrophy spectrum,

$$\Omega_\alpha \equiv \sum_v \Omega_v(\alpha), \quad (4.72)$$

and area spectrum,

$$A_\alpha \equiv \sum_v A_v(\alpha). \quad (4.73)$$

We let these eddies evolve in a field with a Gaussian strain distribution,

$$P(s) = \left( \frac{2}{\pi \langle s^2 \rangle} \right)^{1/2} e^{-s^2/2\langle s^2 \rangle}, \quad (4.74)$$

so that

$$Z_\alpha \equiv \sum_v \langle \eta_v \rangle = \sum_v \int_{\gamma\zeta_v}^\infty s \alpha \Omega_v(\alpha) P(s) ds.$$

Evaluating the integral gives

$$Z_\alpha = \sum_v \alpha \Omega_v(\alpha) \left( \frac{2\langle s^2 \rangle}{\pi} \right)^{1/2} e^{-\gamma^2 \zeta_v^2 / 2\langle s^2 \rangle}. \quad (4.75)$$

To perform the sum over vortices, assume that all the vortices on a particular scale have about the same strength. Then

$$Z_\alpha \approx \alpha \Omega_\alpha \langle s^2 \rangle^{1/2} \Theta \left( \frac{\gamma^2 \Omega_\alpha}{\langle s^2 \rangle A_\alpha} \right), \quad (4.76)$$

with

$$\Theta(\epsilon) = \left( \frac{2}{\pi} \right)^{1/2} e^{-\epsilon}. \quad (4.77)$$

Substituting (4.77) into (4.63) yields

$$\frac{\partial \omega}{\partial \kappa} = \frac{g\epsilon}{\epsilon - 1} - 1, \quad (4.78)$$

which means the root in the denominator is simply  $\epsilon_c = 1$ .

Since  $g$  is a constant in (4.62), integration results in

$$A_\alpha = A_0 \left( \frac{\alpha}{\alpha_0} \right)^{g-1}, \quad (4.79)$$

and gives

$$\epsilon = \frac{\gamma^2}{\langle s^2 \rangle A_0} \left( \frac{\alpha}{\alpha_0} \right)^{1-g} e^{\omega}. \quad (4.80)$$

Use (4.80) to rewrite (4.78) in terms of  $\epsilon$ ,

$$\frac{\partial \epsilon}{\partial \alpha} = \frac{g\epsilon}{\alpha(\epsilon - 1)}, \quad (4.81)$$

which integrates to

$$\epsilon e^{-\epsilon} = \left( \frac{\alpha}{\alpha_0} \right)^{-g} \epsilon_0 e^{-\epsilon_0}. \quad (4.82)$$

In (4.82),  $\epsilon e^{-\epsilon}$  has its global maximum value at  $\epsilon = 1$ , and decays to zero as  $\epsilon \rightarrow 0$  and  $\epsilon \rightarrow \infty$ . So, as the right-hand-side of (4.82) shrinks,  $\epsilon$  will diverge from  $\epsilon_c = 1$ , and as it grows,  $\epsilon$  will converge toward  $\epsilon_c = 1$  until

$$\left( \frac{\alpha}{\alpha_0} \right)^{-g} \epsilon_0 e^{-\epsilon_0} = \frac{1}{e}, \quad (4.83)$$

when there will no longer be a solution. As long as  $g \neq 0$ , there will always be a critical wavenumber,

$$\alpha_c = \alpha_0 (\epsilon_0 e^{1-\epsilon_0})^{1/g}, \quad (4.84)$$

at which there no longer is a solution. If  $g < 0$  there is no solution for  $\alpha > \alpha_c$ , and if  $g > 0$  there is no solution for  $\alpha < \alpha_c$ . Further, note that for any value of  $\alpha$  for which (4.82) has one solution (except for  $\epsilon = 1$ ), it in fact has two: one with  $\epsilon > 1$ , and the other with  $\epsilon < 1$ . Since  $\epsilon_c = 1$  is the critical value of  $\epsilon$ , these two solutions correspond to the coherent structure and background solutions mentioned ear-

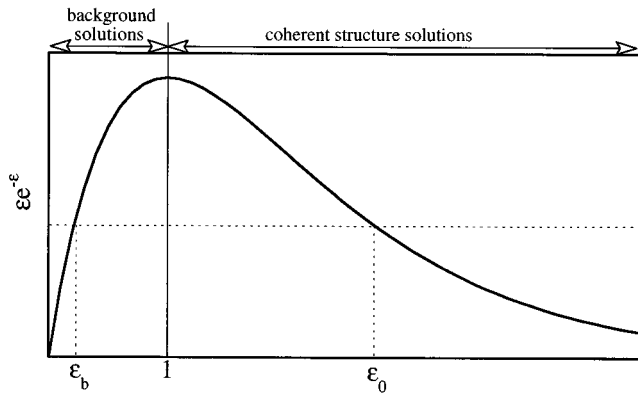


FIG. 3. Graphical view of the coherent structure ( $\epsilon_0$ ) and background ( $\epsilon_b$ ) solutions. For all values of  $\epsilon_0$  determined by (4.86) there is a second solution, save for  $\epsilon_0 = 1$ , which corresponds to the KBL solutions. If  $\epsilon_0 > 1$ , the coherent structures will be at large scales; whereas if  $\epsilon_0 < 1$ , the coherent structures will be at small scales

lier. While one would intuitively look for continuous solutions, in fact since  $\partial \epsilon / \partial \alpha$  is undefined at  $\epsilon = 1$ , jumps between the two solutions are possible.

The properties of a flow in this model can be determined by the non-dimensional enstrophy flux,

$$\theta \equiv \frac{\eta}{\Omega_0 \alpha_0 \langle s^2 \rangle s^{1/2}}; \quad (4.85)$$

$\theta$  can really be seen as a characteristic of the forcing. It is a ratio between the enstrophy put into (or fluxed through) the system, and the strength of the vorticity field at the forcing scale. The ratio will vary with the amount of enstrophy removed from the system and the efficiency with which the forcing injects enstrophy into the system.

The forcing scale intermittence is determined by

$$\epsilon_0 = -\ln \left( \left( \frac{\pi}{2} \right)^{1/2} \theta \right). \quad (4.86)$$

We can then determine the strength of the background flow by finding the other solution to (4.82). If, for simplicity, we let  $g = 0$ , then the background intermittence is determined by solving for the second solution to

$$\epsilon_b e^{-\epsilon_b} = \epsilon_0 e^{-\epsilon_0}; \quad (4.87)$$

a process that is represented graphically by Fig. 3. The strength of the background flow can then be characterized by the value

$$\Omega_b = \frac{\eta \left( \frac{\pi}{2} \right)^{1/2} e^{\epsilon_b}}{\alpha_0 \langle s^2 \rangle s^{1/2}}. \quad (4.88)$$

Solutions to the model fit into three categories:  $0 > \theta > (2/(e^2 \pi))^{1/2}$  where the strong intermittent structures are at large scales (Fig. 4 shows a sample spectrum for this case),  $\theta = (2/(e^2 \pi))^{1/2}$ , with a uniform KBL-like spectrum, and  $(2/(e^2 \pi))^{1/2} > \theta > (2/\pi)^{1/2}$ , where the structures are at small scales.

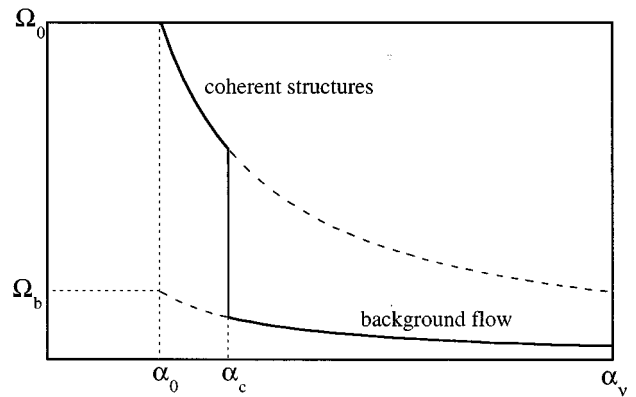


FIG. 4. Schematic plot of an enstrophy spectrum with large-scale coherent structures. The high intermittence at large scales results in a correspondingly strong enstrophy spectrum. There is an abrupt transition to low intermittence, with a weak enstrophy spectrum at smaller scales.

## V. PHENOMENOLOGY AND NUMERICAL STUDIES

The theory presented is by no means a rigorous theory, nor even one that is derived from *a priori* principles. It is not a general theory of non-linear interactions—since it draws from inertial range theory it will not apply to spectrally truncated inviscid simulations. Given those weaknesses (which are shared by many models of turbulence) it still may be useful for explaining the basic phenomenology of the two-dimensional enstrophy cascade.

We examine the theory and compare it to the phenomenology of three different turbulent flows through a brief review of the literature and some numerical simulations. In particular, we will discuss the limits  $\theta \rightarrow 0$  and  $\theta \rightarrow (2/(e^2 \pi))^{1/2}$ , as well as the intermediate case  $0 > \theta > (2/(e^2 \pi))^{1/2}$ . As the theory requires a strong peak in the spectrum at large scales for the interactions to be non-local, it likely that the range  $(2/(e^2 \pi))^{1/2} > \theta > (2/\pi)^{1/2}$  is non-physical.

The  $\theta \rightarrow 0$  limit corresponds to zero enstrophy flux. For this system to be in equilibrium, it must be unforced, leading us to examine the well studied problem of decaying turbulence; i.e. turbulence with viscosity but no forcing and no drag. Since the viscosity removes enstrophy but virtually no energy, the system adjusts to a state of minimum enstrophy for a given energy,<sup>26,4</sup> with zero enstrophy flux through the system. Since the spectrum will still have large scale enstrophy, this means the flow evolves toward infinite intermittence at the large-scale; a process which has been observed in many direct numerical simulations.<sup>17,15,16,25,27,28</sup> The large intermittence grows through vortex mergers resulting in a progressively sparser vorticity field, while the background flow decays to zero and the energy spectrum gets progressively steeper.

We will see that the other two systems correspond to forced vortex turbulence and forced passive scalar dynamics. While the theoretical values of  $\theta$  for these systems are not *a priori* obvious, they can be estimated from the data. The phenomenology presented in the next two sections makes it clear that the passive scalar has the unique KBL-like solution. Forced-dissipative vortex turbulence, on the other hand,

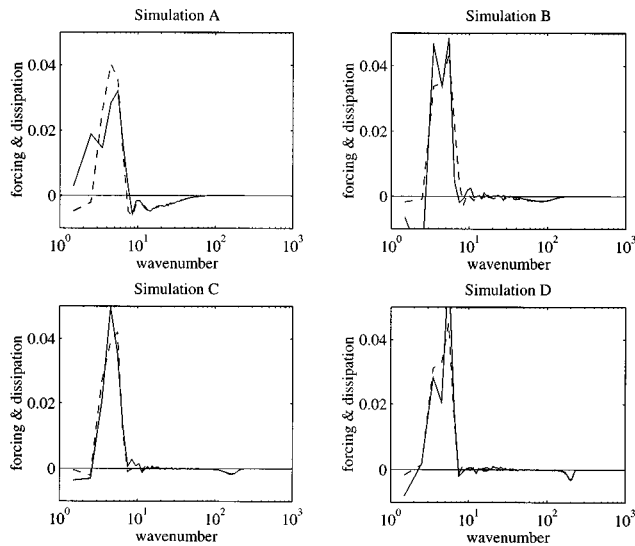


FIG. 5. Sum of (spectral) forcing, viscosity and drag for the passive scalar (dashed line) and vorticity (solid line) for  $\nabla^2$ ,  $\nabla^4$ ,  $\nabla^8$  and  $\nabla^{16}$  viscosities (simulations A–D as referred to in Table I). These two graphs are numerical calculations of the right-hand-side of (2.24) and (2.11) for  $n=1, 2, 4$  and  $8$ . Note that for  $\nabla^2$  viscosity, there is no proper inertial range.

is intermediate between the passive scalar and decaying turbulence, and so, interestingly, has a dual solution with large-scale coherent structures superposed on a small-scale background flow.

### A. Overview of the numerics

Simulations are performed using a de-aliased spectral code of equivalent grid resolution up to  $512 \times 512$ . We enforce an isotropic spectral truncation consistent with this at

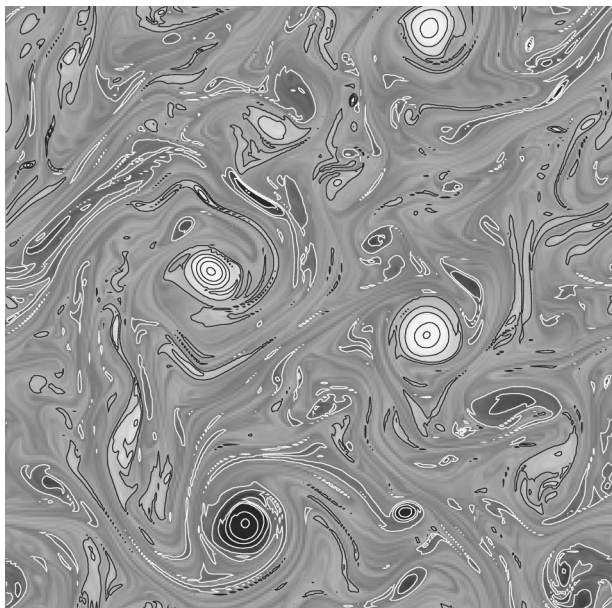


FIG. 6. Image of the instantaneous vorticity field, taken from simulation C in Table I. Dark areas have counterclockwise vorticity and light areas have clockwise vorticity. The contours are placed at integer multiples of the RMS vorticity. Negative contours are black, positive contours are white, and the zero contour has been omitted.

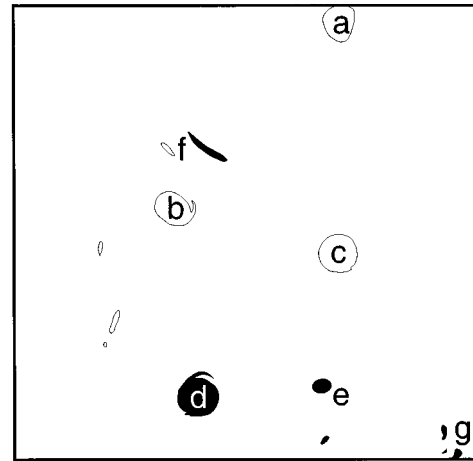


FIG. 7. Key to the features referred to by the text in Figures 6, 8 and 10.

$k_{max}=240$ . The forcing used is Markovian (as in Lilly<sup>29</sup>), typically confined to an annulus of wavenumbers  $4.0 < k < 7.0$ . A drag term is included to remove energy, as well as being appropriate for geophysical applications (i.e., it parameterizes an Ekman layer.)

Figure 5 shows the enstrophy input and removal for a set of four simulations, the first with Newtonian viscosity, and the rest with increasing order hyperviscosities. The two-dimensional analogue of Newtonian viscosity has  $n=2$  in the viscous term in (2.2), but the Newtonian simulation exhibits no inertial range in Fig. 5, the viscous removal of enstrophy overlaps the forcing range. Also, it is not clear that two-dimensional Newtonian viscosity is in fact desirable as a physical model given that geophysical fluids are three-dimensional at the viscous scale. The  $\nabla^4$  hyperviscosity simulation does have a small range of inertial wavenumbers,

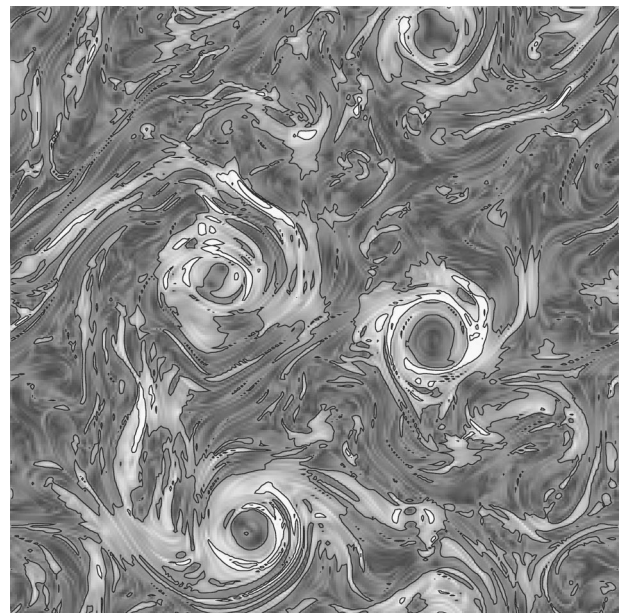


FIG. 8. Image of the instantaneous strain field, taken from simulation C in Table I. The contours are placed at integer multiples of the RMS vorticity.

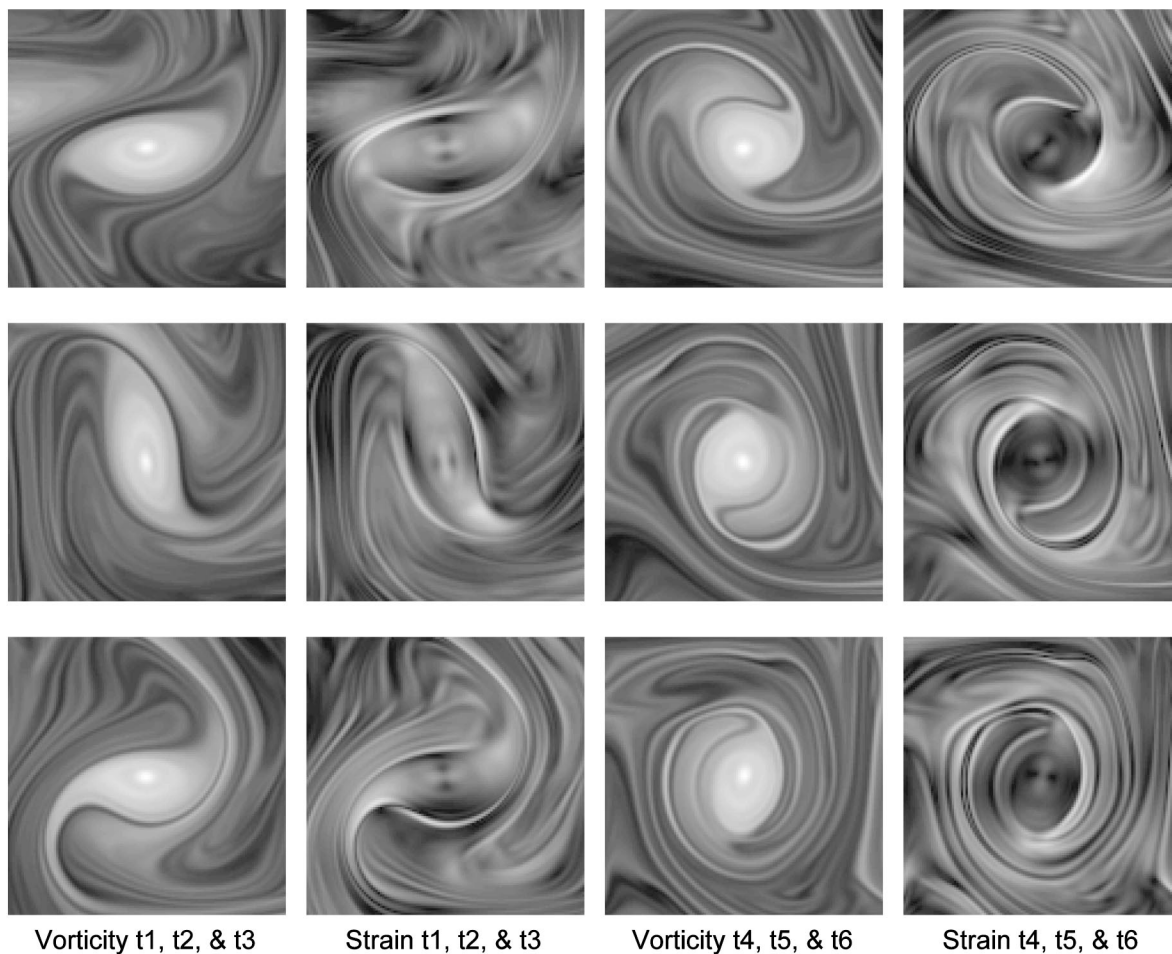


FIG. 9. Time evolution showing the enstrophy transfer from a vortex to the background flow. The images are taken from a larger flow (simulation C in Table I) tracking the vortex as it drifts.

and the higher order hyperviscosities exhibit correspondingly longer inertial ranges.

All simulations are run to equilibrium before any data is taken; the criterion for equilibrium is that the enstrophy input by forcing and removed by viscosity and drag should spectrally match the transfer by the non-linear terms, i.e. the solid and dashed lines in Fig. 5 should match fairly well. Given that simulation C has the lowest order viscosity with a reasonable length inertial range, it was chosen to be the source for most of the remaining data presented. Typical averaging times for the histograms and spectral quantities are 15–20 large-scale eddy turn over times. Note that due to the small quantity of wavenumbers involved in the averages at the largest scales, the spectral properties are only just beginning to converge by this time as one can see from the deviations at the small wavenumbers in Fig. 5.

## B. Real space phenomenology

Much of the physical space phenomenology of the forced two-dimensional enstrophy cascade is visible in Figs. 6, 8 and 10. The structures labeled “a,” “b,” “c,” “d,” and “e” in the key, Fig. 7, are long-lived elliptical coherent structures, all with peak vorticity greater than four times the RMS vorticity of the field. The two structures labeled f are highly eccentric and unstable; they are stretched by the high

strain field visible in Fig. 8. Structure g is the remains of a vortex which has been extended by high strain, and is now rolling back into a smaller vortex. The background flow consists of long continually stretching streamers, and is predominantly weaker than the RMS vorticity.

Figure 9 shows the time evolution of the vorticity and strain of a vortex as it stretches slightly beyond the stable eccentricity limit, sheds vorticity, relaxes to lower eccentricity as the strain drops, and entrains some of the background flow. This is the mechanism of enstrophy flux from the coherent structures to the background flow—the shed streamers become part of the background spectrum, and the entrained background weakens the coherent structure spectrum. In the theory, we use the highly idealized UEV model and a parameterization of this process.

The physical space mechanism for non-locality is apparent in Fig. 8. While the strain is small inside the large-scale vortices, it is strong in a band about it. One of the primary sources of background enstrophy flux is these large-scale bands straining the small-scale flow neighboring the vortices. These bands also serve as a buffer, protecting the core from being distributed by its surroundings.

The passive scalar field, Fig. 10 is superficially similar to the vorticity field at first glance. The contours are similar because the passive scalar eddies are being stretched by the

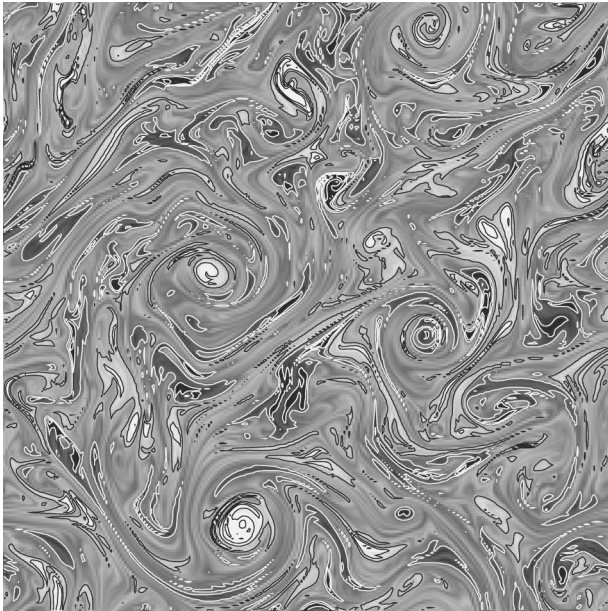


FIG. 10. Image of the instantaneous passive scalar field, taken from simulation C in Table I. The contours are placed at integer multiples of the RMS vorticity. Negative contours are black, positive contours are white and the zero contour has been omitted.

same strain field as the vorticity eddies, but there the similarity stops. The passive scalar is uniform inside the coherent structures because it is trapped on closed streamlines and hence homogenizes, but it is neither particularly strong inside, nor well correlated to the vorticity. For instance, structures “b” and “d” have opposite sign in the vorticity field, but have the same sign in the passive scalar (the passive scalar field is chosen to have zero mean value).

### C. Spectral space phenomenology

As there is no obvious way to compute eddy  $\alpha$  spectra directly, we attempt to verify the theoretical predictions by observing the standard Fourier  $k$  spectra. A field of eddies at a particular scale  $\alpha$  will not, of course, solely have energy at wavenumbers of magnitude  $k$ , rather it will peak around  $k$  with a roll off at smaller wavenumbers determined by the eddy distribution and a roll off at larger wavenumbers determined by the spectral sidebands of the eddy shape. A uniform elliptical vortex has Fourier sidebands that roll off to larger wavenumbers as  $k^{-2}$ ; a real vortex should be somewhat shallower. Given this, the abrupt transition between the coherent structures and the background flow in  $\alpha$  should be masked by the roughly  $k^{-2}$  spectrum of the vortex shapes, but the  $k^{-1}$  background flow should be visible since it rolls off more slowly than the eddy spectrum.

The enstrophy spectra in Fig. 11 show two things clearly, consistent with the theory. The first is the coherent structures at large scales. Above wavenumber  $k=30$  or so, the enstrophy spectrum is steep, with a slope close to  $k^{-2}$ . Below, the enstrophy spectra show a progression toward the theoretically predicted  $k^{-1}$  background spectrum as the inertial range gets longer. [This feature was also noted, but not explained, by Maltrud and Vallis (1991), who noted that it coincided with a peak in a “kurtosis spectrum,” implying that coherent structures existed at larger scales but not at

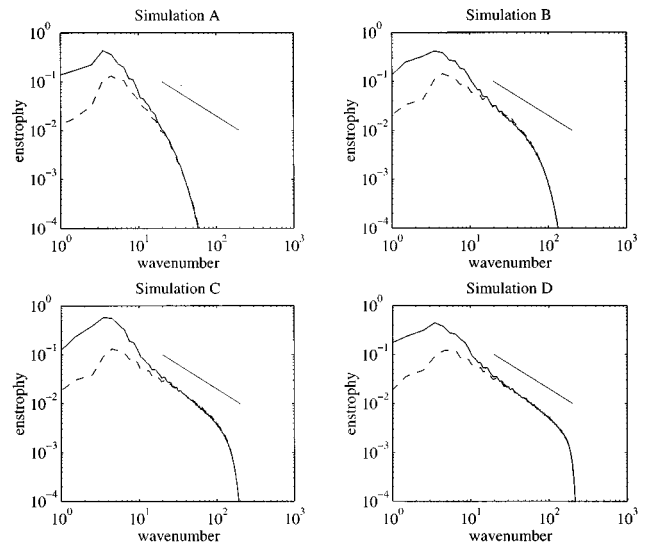


FIG. 11. Passive scalar spectra (dashed line) and enstrophy spectra (solid line) for  $\nabla^2$ ,  $\nabla^4$ ,  $\nabla^8$  and  $\nabla^{16}$  viscosities (simulations A–D as referred to in Table I). The line segments above the spectra show a  $k^{-1}$  spectral slope.

smaller.] The comparison with the passive scalar spectrum makes the transition clear. The passive scalar spectra (in all but simulation A) have the predicted  $k^{-1}$  spectrum at scales below the forcing scale, though they roll off near the viscous scale. The enstrophy spectra are steep at large scales, joining the passive scalar spectrum and progressively getting closer to the  $k^{-1}$  spectrum with a larger wavenumber. Since the passive scalar dynamic is linear, it cannot (for a given velocity field) exhibit transitions between solutions. As argued in Sec. II B, when the spectrally non-local terms dominate (i.e., at small scales) the dynamics of the vorticity and the passive scalar are equivalent, and both give a  $k^{-1}$  spectrum. The coherent structures in the vorticity field exist at larger scales where the spectra diverge. The bend in the enstrophy spectrum around wavenumber 30 is the spectral manifestation of the transition between the coherent structure solution and the background solution.

The close match up between the coherent structure spectrum in Fig. 11 and the ideal UEV spectrum of  $k^{-2}$  is rather serendipitous. The actual vortices in the DNS are closer to a Gaussian shape than to a UEV, so their spectra will be exponential. In these forced simulations, the vortex spectrum is observable over at most two octaves in scale, so it is difficult to conclude much about it from Fig. 11.

To compare the theory and DNS, we examine the non-dimensional inverse rate of strain,

$$I_k = \frac{\Omega^{1/2}}{\sigma_k} = \frac{k\Omega_k\Omega^{1/2}}{Z_k}, \quad (5.89)$$

and its equivalent for the passive scalar,

$$\tilde{T}_k = \frac{k\Phi_k\Omega^{1/2}}{\tilde{Z}_k}, \quad (5.90)$$

$I_k$  is a proxy for  $\Theta_\alpha^{-1}$  in the sense that it will be large for scales where intermittence is high and the local terms dominate, and small for scales where intermittence is low and

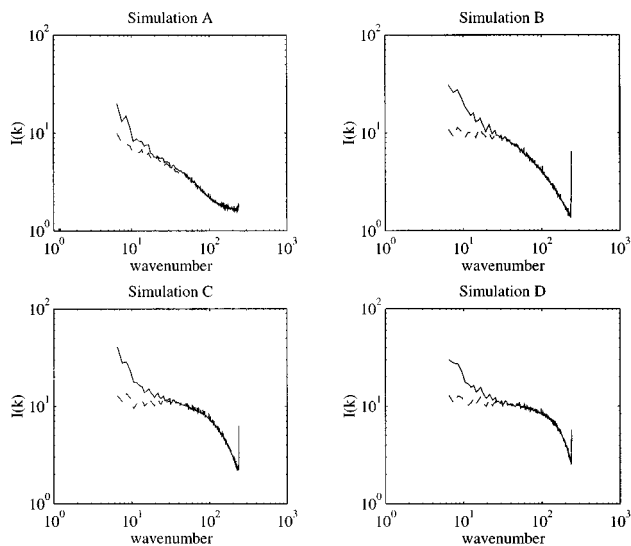


FIG. 12. Inverse strain rate [defined in (5.89)] for the passive scalar (dashed line) and vorticity (solid line) for  $\nabla^2$ ,  $\nabla^4$ ,  $\nabla^8$ , and  $\nabla^{16}$  viscosities (simulations A–D as referred to in Table I). The smallest wavenumber plotted is  $k=7$  because the strain rate is not well defined in the forcing region. The spikes at the high wavenumber end of the spectrum are due to the finite truncation scale.

non-local terms dominate. If one takes the correspondence between (5.89) and its equivalent for  $\Theta$ , (4.76), literally, then (4.77) gives simply

$$I_k = (\pi/2)^{1/2} e^{\epsilon k}. \quad (5.91)$$

The inverse rates of strain in Fig. 12 also show the transition between the coherent structures and the background flow. As one would expect,  $\tilde{I}_k$  is nearly flat for the first decade smaller than the forcing scale. By contrast, from wavenumber 30 to the forcing scale,  $I_k$  turns toward higher intermittence. The gradual transition between coherent structures and the background flow reflects the  $k^{-2}$  spectrum of the coherent vortices. Beyond wavenumber 30, both  $I_k$  and  $\tilde{I}_k$  are nearly flat in simulation D, until the dissipation scale is reached.

A key point in the theory presented in Sec. IV is the relationship between spectral measures like  $I_k$  and spatial measures of intermittence. Without an unambiguous way to decompose the vorticity into an eddy-like (rather than Fourier) basis, a quantitative relationship is difficult to demonstrate. Nonetheless, a comparison between the vorticity and passive scalar PDFs, Fig. 2 shows that while the passive scalar is not completely Gaussian, it does not exhibit the high intermittence extrema of the vorticity field. The coherent structures in Fig. 6 are clearly responsible for the long tail in the vorticity PDF. We suggest that the spacial intermittence of the persistent vorticities results in the increased value of  $I_k$  at large scales and the steeper than  $k^{-1}$  enstrophy spectrum in the wavenumber regime close to the forcing scale.

#### D. Discussion on the numerical results

The mean strain field model makes several predictions about the two-dimensional enstrophy cascade: that there will be abrupt transitions between coherent structures and back-

ground flow, that the background flow will behave like a passive scalar, that the foreground and background flows will each have  $\alpha^{-1}$  enstrophy spectra, and that observed Fourier spectra steeper than  $k^{-1}$  are due to the transition between the two solutions. On the first two counts, the theory does quite well. The data presented show a clear high intermittence coherent structure field at large scales rolling off rapidly into a background flow which is spectrally indistinguishable from the passive scalar.

The theory predicts a  $\alpha^{-1}$  slope in the range of coherent structures, but since the structures only exist over a small range in scales near the forcing, the actual slope is not visible in the Fourier spectrum; the  $k^{-2}$  enstrophy slope observed is likely some combination of the exponential roll off of the vortices and the actual vortex spectrum. If we look at the problem in physical space, an  $\alpha^{-1}$  slope corresponds to a field where eddies of all scales have the same strength. In Fig. 6, the largest vortices do have roughly the same strength, although we have not undertaken a sophisticated census.

For the background flow, and scales smaller than the coherent structures, the theory predicts an  $\alpha^{-1}$  spectrum, corresponding to a constant value for  $I_k$ , for the vorticity background flow and for the entire inertial range of the passive scalar. The numerics are consistent, if not conclusive. In Fig. 12, the actual spectra start rolling off at scales larger than the viscous scale. While  $I_k$  is indeed constant at large scales in the passive scalar, the transition to the coherent structure solution begins before the spectrum has a chance to completely flatten out. The difficulty is that the effects of the viscosity intrude a long way into larger scales.

The mean strain field model is based on the hypothesis that the small-scale dynamics are not sensitive to the size of the large-scale structures. As a result, we concluded that the background flow and passive scalar must have  $\alpha^{-1}$  spectra because the enstrophy flux could only depend on the local wavenumber, even though it depends on the strength of the large-scale flow. The data presented are consistent with this assumption because the small-scale  $k$  dependence of  $I_k$  seems to involve the viscous scale, not the forcing scale.

#### VI. CONCLUSIONS

The theoretical work in this paper utilizes the basic ideas of inertial range theory, and extends them phenomenologically by incorporating ideas of vortex–strain interactions that are normally presented in physical and not spectral space. In particular, we classify or parameterize the variety of enstrophy cascades by a single non-dimensional parameter  $\theta$  defined in (4.85). This parameter is essentially a ratio of the enstrophy flux in the cascade to the RMS strain in the flow, and in the theory reflects the strength and intermittence of the coherent structures in the flow.

One extreme of this classification system is  $\theta=0$ , corresponding to the weak enstrophy flux of freely decaying turbulence. Decaying turbulence is well studied in the literature, exhibiting very strong coherent structures and extremely high intermittence. The other extreme,  $\theta \sim 1$ , is the passive scalar, with no coherent structures and a nearly Gaussian distribution of scalar field. Turbulence forced by a random

process, with enstrophy removal at a much smaller scale and energy removal at a larger scale forms an intermediate case. These solutions have a well defined field of coherent structures at large scales and a discrete transition to a low intermittence background flow.

From a physical standpoint, the presence or otherwise of coherent vortices depends on their strength relative to the mean straining field, and the dynamics of vortex merger suggest that vortices will exist where they can. In forced turbulence, vortices at or slightly smaller than the forcing scale are strong enough to survive the straining field, and a rather steep spectrum ensues, dominated by the spectrum of the vortices themselves. At smaller scales, the necessarily weaker vortices cannot survive the strain, and an enstrophy spectrum of the classical  $k^{-1}$  form results. The dynamics of passive scalar turbulence are similar to the dynamics at the small scales of forced vortex turbulence, with low intermittence, a near Gaussian distribution of vorticity or passive scalar, and the classical  $k^{-1}$  spectrum, even though the non-linear interactions remain spectrally non-local. At these small scales the vorticity is essentially a passive scalar. In decaying vortex turbulence the enstrophy flux is minimal after the background field is cascaded away, and vortices can dominate over the weak straining field producing a generally steep spectrum, many vortices and a highly intermittent structure.

Borue<sup>8</sup> has performed simulations at higher resolution than those reported here. These simulations show a steeper energy spectrum near the forcing scale, but a spectrum quite close to  $-3$  away from that region. These results also have a non-local enstrophy transfer, even in the region where the classical  $-3$  spectrum holds. The number of large coherent vortices in the simulations seems roughly proportional to the forcing scale, rather than populating the entire enstrophy spectrum. These results are all consistent with the model presented in this paper.

In sum, while the mean strain field theory is far from a complete description of dynamics of the enstrophy cascade, we think it provides some insight into the basic phenomenology of two-dimensional turbulence, and an interpretation for non-classical spectra, intermittence and coherent structures. The theory makes certain predictions, all of which are consistent with the preliminary numerical work presented here and simulations of others. Further, if a sufficiently high resolution simulation of two-dimensional turbulence could be performed, an inertial range spectrum with a  $k^{-3}$  energy spectrum should be observed (at scales far from the forcing) even with a conventional Newtonian viscosity. The spectrum of a passive scalar forced in the same way as vorticity should also lie on top of the enstrophy spectrum at scales far from the forcing scale. Current simulations do already give some hint of this.

## ACKNOWLEDGMENTS

This work was funded by the NSF.

<sup>1</sup>R. H. Kraichnan, "Inertial ranges in two-dimensional turbulence," *Phys. Fluids* **10**, 1417 (1967).

- <sup>2</sup>C. E. Leith, "Diffusion approximation for two-dimensional turbulence," *Phys. Fluids* **11**, 671 (1968).
- <sup>3</sup>G. K. Batchelor, "Computation of the energy spectrum in two-dimensional turbulence," *Phys. Fluids. Suppl. II* **12**, 233 (1969).
- <sup>4</sup>R. H. Kraichnan and D. Montgomery, "Two dimensional turbulence," *Rep. Prog. Phys.* **43**, 571 (1980).
- <sup>5</sup>G. K. Vallis, "Problems and phenomenology in two-dimensional turbulence," in *Nonlinear Phenomena in the Atmospheric and Oceanic Sciences*, edited by G. Carnevale and R. Pierrehumbert (Springer-Verlag, New York, 1992), pp. 1–25.
- <sup>6</sup>K. Ohkitani, "Nonlocality in a forced two-dimensional turbulence," *Phys. Fluids A* **2**, 1529 (1990).
- <sup>7</sup>M. E. Maltrud and G. K. Vallis, "Energy and enstrophy transfer in numerical simulations of two dimensional turbulence," *Phys. Fluids A* **5**, 1760 (1993).
- <sup>8</sup>V. Borue, "Spectral exponents of enstrophy cascade in stationary two-dimensional homogeneous turbulence," *Phys. Rev. Lett.* **71**, 3967 (1993).
- <sup>9</sup>A. N. Kolmogorov, "A refinement of previous hypotheses concerning the local structure of turbulence in a viscous incompressible fluid at high Reynolds number," *J. Fluid Mech.* **13**, 82 (1962).
- <sup>10</sup>B. Fornberg, "A numerical study of 2d turbulence," *J. Comput. Phys.* **25**, 1 (1977).
- <sup>11</sup>J. C. McWilliams, "The emergence of isolate coherent vortices in turbulent flow," *J. Fluid Mech.* **146**, 21 (1984).
- <sup>12</sup>M. E. Maltrud and G. K. Vallis, "Energy spectra and coherent structures in forced two-dimensional and beta-plane turbulence," *J. Fluid Mech.* **228**, 321 (1991).
- <sup>13</sup>R. H. Kraichnan, "Inertial-range transfer in two- and three-dimensional turbulence," *J. Fluid Mech.* **47**, 525 (1971).
- <sup>14</sup>R. Benzi, S. Patarnello, and P. Santangelo, "Self-similar coherent structures in two-dimensional decaying turbulence," *J. Phys. A* **21**, 1221 (1988).
- <sup>15</sup>W. H. Matthaeus, W. T. Stribling, D. Martinez, S. Oughton, and D. Montgomery, "Selective decay and coherent vortices in two-dimensional incompressible turbulence," *Phys. Rev. Lett.* **66**, 321 (1991).
- <sup>16</sup>W. H. Matthaeus, W. T. Stribling, D. Martinez, S. Oughton, and D. Montgomery, "Decaying, two-dimensional, Navier-Stokes turbulence at very long times," *Physica D* **51**, 531 (1991).
- <sup>17</sup>J. C. McWilliams, "A demonstration of the suppression of turbulent cascades by coherent vortices in two-dimensional turbulence," *Phys. Fluids A* **2**, 547 (1989).
- <sup>18</sup>P. Bartello and T. Warn, "Self-similarity of decaying two-dimensional turbulence," *J. Fluid Mech.* **326**, 357 (1996).
- <sup>19</sup>A. Babiano, C. Basdevant, B. Legras, and R. Sadourny, "Vorticity and passive-scalar dynamics in two-dimensional turbulence," *J. Fluid Mech.* **183**, 379 (1987).
- <sup>20</sup>K. Ohkitani, "Wave number space dynamics of enstrophy cascade in a forced two-dimensional turbulence," *Phys. Fluids A* **3**, 1598 (1991).
- <sup>21</sup>S-K Ma, *Modern Theory of Critical Phenomena* (Benjamin/Cummings, Reading, MA, 1976).
- <sup>22</sup>J. Weiss, "The dynamics of enstrophy transfer in two-dimensional hydrodynamics," *Physica D* **48**, 273 (1991).
- <sup>23</sup>D. W. Moore and P. G. Saffman, "Structure of a line vortex in an imposed strain, in *Aircraft Wake Turbulence and Its Detection* (Plenum, New York, 1971), pp. 339–354.
- <sup>24</sup>S. Kida, "Motion of an elliptic vortex in a uniform shear flow," *J. Phys. Soc. Jpn.* **50**, 3517 (1981).
- <sup>25</sup>G. F. Carnevale, J. C. McWilliams, Y. Pomeau, J. B. Weiss, and W. R. Young, "Evolution of vortex statistics in two-dimensional turbulence," *Phys. Rev. Lett.* **66**, 2735 (1981).
- <sup>26</sup>W. H. Matthaeus and D. Montgomery, "Selective decay hypothesis at high mechanical and magnetic Reynolds numbers," *Ann. (N.Y.) Acad. Sci.* **357**, 203 (1980).
- <sup>27</sup>D. Montgomery, W. H. Matthaeus, W. T. Stribling, D. Martinez, and S. Oughton, "Relaxation in two dimensions and the sinh-Poisson equation," *Phys. Fluids A* **3**, 3 (1992).
- <sup>28</sup>D. Montgomery, X. Shan, and W. H. Matthaeus, "Navier-Stokes relaxation to sinh-Poisson states at finite Reynolds numbers," *Phys. Fluids A* **5**, 2207 (1993).
- <sup>29</sup>D. K. Lilly, "Numerical simulation of two-dimensional turbulence," *Phys. Fluids Suppl. II* **2**, 240 (1969).